Carbohydrate Polymers 137 (2016) 426–432

Contents lists available at ScienceDirect

Carbohydrate Polymers

journal homepage: www.elsevier.com/locate/carbpol

Characterization of un-plasticized and propylene carbonate plasticized carboxymethyl cellulose doped ammonium chloride solid biopolymer electrolytes

N.H. Ahmad, M.I.N. Isa *

School of Fundamental Science, Universiti Malaysia Terengganu, 21030 Kuala Terengganu, Terengganu, Malaysia

ARTICLE INFO

Article history:
Received 23 August 2015
Received in revised form 27 October 2015
Accepted 29 October 2015
Available online 2 November 2015

Keywords:
Carboxymethyl cellulose
Ammonium chloride
Propylene carbonate
Solid biopolymer electrolytes
Ionic conductivity
Plasticizer

ABSTRACT

Two solid biopolymer electrolytes (SBEs) systems of carboxymethyl cellulose doped ammonium chloride (CMC-AC) and propylene carbonate plasticized (CMC-AC-PC) were prepared via solution casting technique. The ionic conductivity of SBEs were analyzed using electrical impedance spectroscopy (EIS) in the frequency range of 50 Hz–1 MHz at ambient temperature (303 K). The highest ionic conductivity of CMC-AC SBE is 1.43×10^{-3} S/cm for 16 wt.% of AC while the highest conductivity of plasticized SBE system is 1.01×10^{-2} S/cm when added with 8 wt.% of PC. TGA/DSC showed that the addition of PC had increased the decomposition temperature compared of CMC-AC SBE. Fourier transform infrared (FTIR) spectra showed the occurrence of complexation between the SBE components and it is proved successfully executed by Gaussian software. X-ray diffraction (XRD) indicated that amorphous nature of SBEs. It is believed that the PC is one of the most promising plasticizer to enhance the ionic conductivity and performance for SBE system.

1. Introduction

In the 20th century, plethora of polymers has been used as structural materials or electric insulators. But, in recent years, researchers have been creating an electrolyte from combination between ion conductors and appropriate salts. Wright had reported (Wright, 1975) that polymer plays a role as a host for appropriate salt, therefore creating a solid polymer–salt complex electrolyte.

Nowadays, solid biopolymer electrolyte (SBE) system has achieved a lot of attraction all over the world since it shows a great prospect in application of electrochemical devices. SBE plays an important role in solid state ionics due to their distinctive properties, such as ease of fabrication, good electrode–electrolyte contact and good dimensional, thermal stability, able to accommodate a wide range of ionic salt doping compositions and high ionic conductivity (Rani, Rudhziah, Ahmad, & Mohamed, 2014; Sohaimy & Isa, 2015). Carboxymethyl cellulose (CMC) is chosen as polymer hosts due to lower cost, in an environmental friendly manner and with good chemical and physical properties (Rozali & Isa, 2014; Zhang, Liu, Cui, & Chen, 2015). CMC is one type of cellulose polymers that has been widely used in a diverse array of application, for example in paper, food additives, textiles fibers, adhesives, paints, pharmaceuticals, cosmetics and medical supplies (Yokota, Ueno, Kitaoka, & Wariishi, 2007). It is natural organic polymer that the most abundant bio-macromolecule, biocompatible and biodegradable (Kamarudin & Isa, 2013). It contains a hydrophobic polysaccharide backbone and many hydrophilic carboxyl groups; hence, showing amphiphilic characteristic (Chai & Isa, 2011).

In order to obtain high ionic conductivity SBE films, several methods had been used such as blending, copolymerization, addition of ceramic fillers (Sekhar, Kumar, & Sharma, 2012) and etc. Besides, one of the methods in increasing the ionic conductivity is plasticizing the film with suitable amount of plasticizer. There was many plasticizers that had been commercialized such as ethylene carbonate (EC), propylene carbonate (PC), polyethylene glycol (PEG), dimethyl carbonate (DMC), diethyl carbonate (DEC) and etc. (Ng & Mohamad, 2006). These plasticizers were chosen based on a few properties such as, high dielectric constant, help to enhance the ionic dissociation, low viscosity, decrease the glass transition and increase the amorphous content (Ahmad, Isa, & Osman, 2011; Pradhan, Choudhary, & Samantaray, 2008; Samsudin & Isa, 2013). Previous work (Suthanthiraraj & Vadivel, 2012; propylene carbonate (PC)) has been chosen as the plasticizer since it has high dielectric constant, $\varepsilon = 64.4$ (Pitawala, Dissanayake, Seneviratne, Mellander, & Albinson, 2008). In addition, PC is highly soluble with CMC and AC.

* Corresponding author. Tel.: +60 96683111.
E-mail address: ikmar.isa@umt.edu.my (M.I.N. Isa).

http://dx.doi.org/10.1016/j.carbpol.2015.10.092
0144-8617/

The present work aimed to investigate the electrical, structural and nature behavior of the SBEs system by using electrical impedance spectroscopy (EIS), Fourier Transform Infrared (FTIR) Spectroscopy, X-ray Diffraction (XRD), Differential Scanning Calorimetry (DSC) and Thermogravimetric analysis (TGA). Analysis on absorption of FTIR spectra will be compared using Gaussian simulation software. These experiment combination techniques give in deep understanding on the SBE behavior.

2. Experimental

2.1. Sample preparation

2.0 g of CMC (Acros Organic Co.) was added into distilled water and stirred until it was completely dissolved. Different amount of AC was added to the CMC solution and stirred again until the solutions became homogeneous. The mixture was cast into petri dish and heated in an oven at constant temperature of 50 °C for 14 hours. Then, the films were kept into desiccator (with silica gel) for further drying. For the plasticized sample, the highest conductivity of CMC-AC SBE was chosen to be added with plasticizer. The same method was used to produce CMC-AC-PC SBEs by adding different amount of propylene carbonate (PC) as plasticizer into CMC-AC mixture as captured into Table 1.

2.2. Sample characterization

2.2.1. Electrical impedance spectroscopy (EIS)

The ionic conductivity of SBEs were investigated by electrical impedance spectroscopy (EIS) similarly done by other workers (Ramesh, Shanti, & Morris, 2012; Taib & Idris, 2014; Ali, Yahya, Bahron, & Subban, 2007; Shukur, Ithnin, & Kadir, 2014; Sreenivasachari, 2013) using HIOKI 3532-50 LCR Hi-Tester in the frequency range of 50 Hz to 1 MHz at temperatures from 303 K to 353 K. SBE was placed between two stainless steel electrodes of a conductivity cell which connected to a computer. A graph of negative imaginary impedance against real impedance known as Cole–Cole plot was then obtained. From the bulk resistance (R_b) value can be determined from the Cole–Cole plots. The ionic conductivity (σ) was calculated using the following equation (Ramesh et al., 2012; Taib & Idris, 2014; Ali et al., 2007; Shukur et al., 2014; Sreenivasachari, 2013):

$$\sigma = \frac{t}{R_b A} \quad (1)$$

where t (cm) is the thickness and A (cm^2) is the electrode–electrolyte contact area of SBEs.

Table 1
Designation of SBEs.

Designation	Formulation				
	CMC (g)	AC (wt.%)	AC (g)	PC (wt.%)	PC (g)
A0	2	0	0.000	0	0
A4		4	0.083		
A8		8	0.174		
A12		12	0.273		
A16		16	0.381		
A20		20	0.500		
B2	2	16	0.381	2	0.041
B4				4	0.099
B6				6	0.152
B8				8	0.207
B10				10	0.265
B12				12	0.325

2.2.2. Differential scanning calorimetry (DSC)

The thermal properties of the SBEs were determined by differential scanning calorimetry (DSC) (Model Mettler—Toledo (TGA/DSC) equipped with star^e system). ~30 mg of SBEs were placed on aluminum pan of DSC equipment. Empty pan was used as the reference. The glass transition temperature (T_g) of the different SBEs were measured at a heating scan rate of 10 °C/min from 30 °C to 400 °C.

2.2.3. Thermogravimetric analysis (TGA)

TGA was carried out using Mettler—Toledo (TGA/DSC) equipped with star^e system to determine the decomposition temperature and information regarding of the water content in the SBEs. About ~30 mg of the sample was sealed into aluminum pans and heated from 30 to 400 °C under argon flow at a heating rate of 10 °C/min.

2.2.4. X-ray diffraction (XRD)

XRD was carried out to determine the effect of Cu$K\alpha$ on the nature of the samples. X-ray diffractograms of all samples were recorded using an X-ray Diffractometer from 2θ angle about 5 to 60°.

2.2.5. Fourier transform infrared (FTIR) spectroscopy

The complexation of SBEs can be determined by using Fourier Transform Infrared spectroscopy. A Thermo Nicolet 380 FTIR spectrometer equipped with an Attenuated Total Reflection (ATR) accessory utilizing a germanium crystal. The spectrum was recorded in the frequency ranging between 4000 and 700 cm^{-1} with a resolution of 4 cm^{-1}.

2.2.6. Computational

The Gaussian 09W program and method B3LYP were used in order to perform geometry optimizations and frequency calculations on a large set of molecules. These optimization and frequency calculations were made for the 6-31G basis set.

3. Results and discussions

The free-standing of SBEs with good mechanical property is shown in Fig. 1.

3.1. Assessment of compatibility of A0, A16 and B8 SBEs by conductivity, TGA and DSC studies

Fig. 2 shows the Cole–Cole plot of the highest conducting SBE for A16 and B8 at ambient temperature (303 K). Inset figure (A0) shows a tilted semicircle implying that the material is partially resistive and capacitive. However, A16 and B8 SBEs are very capacitive in nature. The capacitance of these two SBEs changes with frequency. The reduced semicircle and inclined spike can be related to the increment in ionic mobility and the number of charge carriers of free ions (H^+) (Ahmad & Isa, 2015a) proven by FTIR analysis. R_b value for SBEs were determined from the intercept of high-frequency semi-circle and low frequency spike on Z_r-axis as shown in Fig. 2.

Table 2 showed the ionic conductivity for A0, A16 and B8 SBEs system. It shows that B8 has the highest ionic conductivity compared to A16 and A0 SBEs. This is due to the addition of propylene carbonate as plasticizer. This trend before and after added with plasticizer was similar to the result obtained by (Pitawala et al., 2008). As a certain amount of plasticizer added, more protons (H^+) are supplied due to the dissociation of the ion (Kumar, Tiwari, & Srivastava, 2012). The contribution to the ionic conductivity enhancement for plasticized SBEs were due to increase in the segmental mobility of polymer chains (Sekhar et al., 2012).

The temperature dependence of the ionic conductivity for A0, A16 and B8 SBEs system is shown in Fig. 3. It is observed that

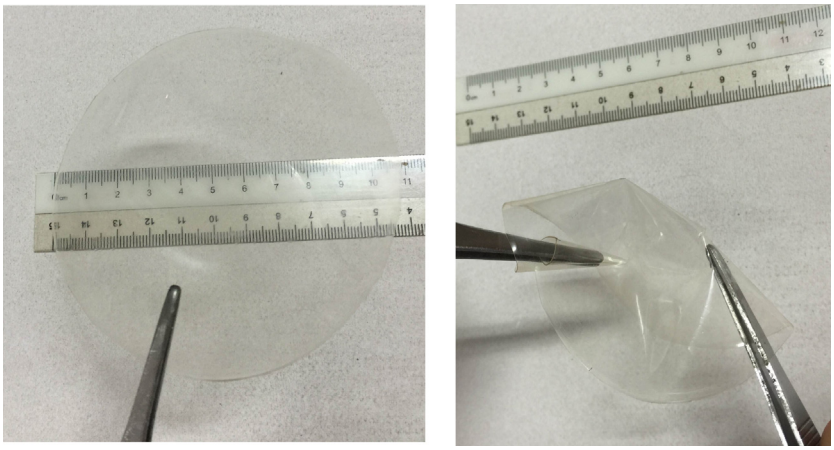

Fig. 1. Clear, transparent and good mechanical properties of SBE.

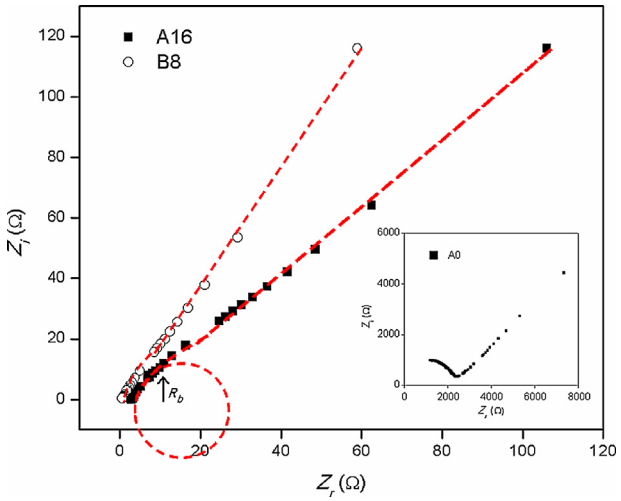

Fig. 2. Cole–Cole plot for A16 and B8 SBEs. Inset: Cole–Cole plot for A0 SBE.

Table 2
Thickness and bulk resistance for A0, A16 and B8 SBEs.

SBE	Thickness, t (cm)	Bulk resistance, R_b (Ω)	Conductivity, σ (S/cm)
A0	0.010	24,900.00	$(1.11 \pm 0.04) \times 10^{-7}$
A16	0.012	2.82	$(1.43 \pm 0.02) \times 10^{-3}$
B8	0.020	0.63	$(1.01 \pm 0.003) \times 10^{-2}$

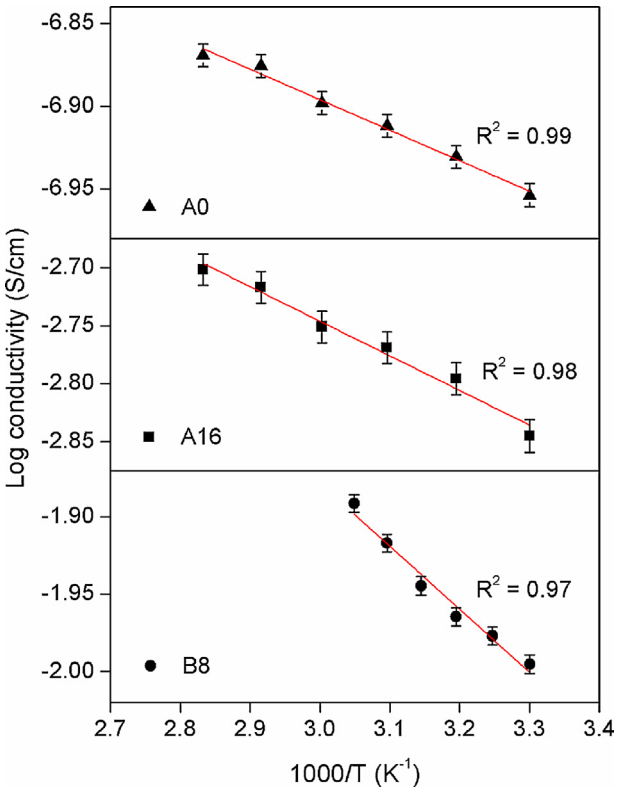

Fig. 3. Temperature dependent conductivity for 303–353 K of SBEs system (Interval 10 K for A0 and A16, interval 5 K for B8).

the regression values for A0, A16 and B8 have been found to be close to unity, suggesting that the temperature dependent ionic conductivity for all the complexes obeys the Arrhenius relation. A comparable Arrhenian conductivity–temperature relationship has been observed in other system i.e. PVA–NH_4Cl, PVA–NH_4Br and PVA–NH_4I (Hema, Selvasekarapandian, Arunkumar, Sakunthala, & Nithya, 2009; Hema, Selvasekerapandian, & Hirankumar, 2007). Previous workers (Rajendran, Sivakumar, & Subadevi, 2003) reported that the sample with plasticizer (EC) gives the optimum value of 1.29×10^{-3} S/cm and the conductivity–temperature plot is Arrhenian. The conductivity and temperature dependent in this work also comparable with Rajendran and co-workers. In current work, no abrupt jump in conductivity value with temperature can be seen in each SBEs system. This indicates that the SBEs exhibit a completely amorphous structure (Ravi et al., 2011). From the plot, it is evident that as the temperature increases the ionic conductivity increases for all SBEs system similar temperature behavior has been reported by (Kadir, Teo, Majid, & Arof, 2009). The increase in conductivity with temperature may be due to the decrease in viscosity which increased chain flexibility (Saroj & Singh, 2012). The temperature range for present work is 303–353 K (10 K increment) for A16 and 303–328 K (5 K increment) for B8 SBE. These selected temperature ranges were selected based from the DSC result.

In order to determine glass transition temperature, T_g, DSC analysis has been implemented. Fig. 4 shows the DSC thermogram of A0 (inset), A16 and B8 SBEs in temperature range of 30–400 °C. At T_g, a small endothermic reaction will be observed in the specific heat of the sample increases. It shows a different feature in the A16 and B8 DSC thermograms having one endothermic at 56.89 °C and others peak at relatively higher temperatures due to the decomposition of the main chain. This step is followed by depolymerization, which proceeds due to the cleavage of glycosidic linkages (Ramesh & Arof, 2001). The other small exothermic peaks at 300.93 °C and

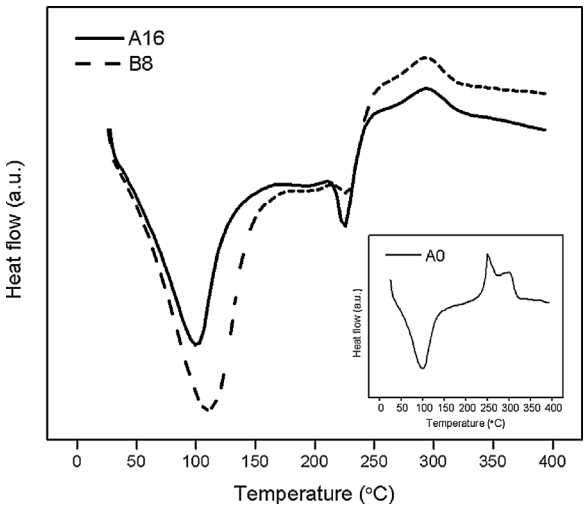

Fig. 4. DSC thermograms of A16 and B8 SBEs. Inset: DSC thermogram for A0 SBE.

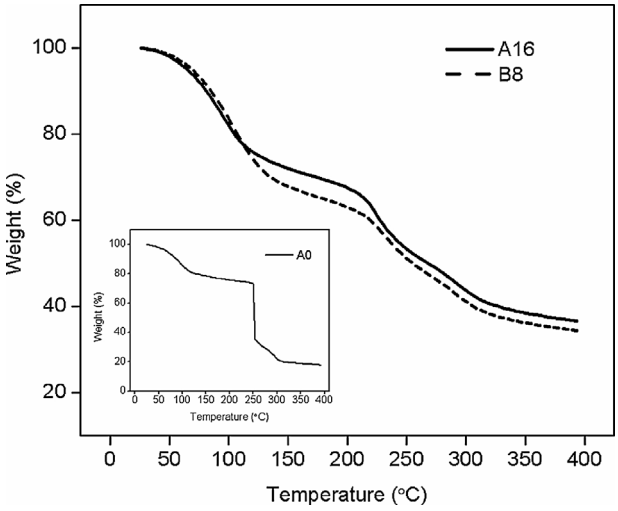

Fig. 5. TGA thermograms of A16 and B8 SBES. Inset: TGA thermogram for A0 SBE.

above are due to the combustion of the degraded SBEs. These two temperature results were similar with the works reported by (Su, Huang, Yuan, Wang, & Li, 2010; Samsudin, Lai, & Isa, 2014). The instability of 1st endothermic peak of SBEs observed is the presence of water contained in CMC by itself (Liu, Yu, Liu, Chen, & Li, 2009). 1st endothermic thermal degradation of CMC take places due to the evaporation of residual solvent, moisture and impurities which mainly referring to the designated molecule of O—H in CMC backbone. Biopolymer tends to absorb moisture from its surrounding and contributes in the initial weight loss (Samsudin et al., 2014). 2nd endothermic thermal degradation of SBEs, B8 was found to be lower than A16. It is due to a lubricating effect (Morales & Acosta, 1997). The decrease in T_g helps to soften the polymer backbone and increase its segmental motion. Theoretically, easy flow of the polymer chains can increase the ionic conductivity. It's proven by conductivity result in Table 2. Current work exhibited similar trend by (Pradhan, Choudhary, Samantaray, Karan, & Katiyar, 2007) using PEG as plasticizer. The addition of PC as plasticizer gives a major contribution to the enhancement in conductivity that comes from the structural changes associated with polymer host (Johan & Ting, 2011).

Fig. 5 shows the TGA thermograms of A0, A16 and B8 SBEs. Su et al. reported that water was evaporated and degradation process occurred at 50 to 150 °C (Su et al., 2010). In this region, A0 SBE exhibits −19% weight loss. The second stage of the degradation was melting temperature, T_m ranging from 250 to 300 °C represent the volatilization of the easily degraded components. As reported by (Su et al., 2010), CMC decomposes in a two-stage process. The initial weight loss is attributed to the presence of a small amount of moisture influenced from the uses of distilled water as solvent in SBE system and the second weight loss looks extreme drop arises due to CO_2 from the COO— groups. Above 300 °C, CMC start to decompose.

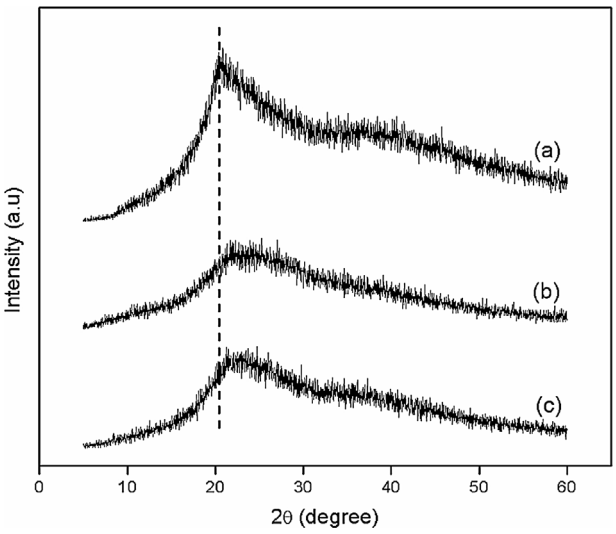

Fig. 6. XRD patterns for (a) A0 (b) A16 (c) B8 SBEs.

For A16 and B8 SBEs, it can be observed the first weight loss is higher (~27–31%) than A0 SBE. This result was higher due to water retention abilities in plasticized sample and containing salt compared to the A0 (Ramesh et al., 2012). It is certainly because of hydrophilic nature of ionic dopant and plasticizer (Shukur et al., 2014). First stage of decomposition temperature for A16 can be observed less than 100 °C. This observation tells the decline in the heat resistivity results from the disruption of strong hydrogen bonding network in A16 (Rani et al., 2014). In this present work, addition of AC in CMC SBE shows an improvement in both the heat-resistivity and thermal stability of A0 SBE. With addition of AC, the maximum decomposition temperature, T_d increases while the total weight loss of the SBE decreases and achieved the highest T_d at temperature 320.29 °C with total weight loss 38.26% for A16 SBE. This is attributed to the complexation of proton (H^+) from NH_4Cl with COO— group of CMC backbone. However, the heat resistivity of B8 decreases compared to A16. This is because propylene carbonate weakens the interaction among polymer chain in a greater extent compared to ammonium chloride. This causes an immense increase in the structural disorderliness in carboxylate anion (COO^-) from CMC, thus minimum amount of heat is sufficient to decompose the polymer electrolytes (Ramesh et al., 2012). Hereby, addition of plasticizer will make the matrix increasingly lose its resistivity toward heat and gradually decreases the decomposition temperature. The un-plasticized SBE and plasticized SBE by using same plasticizer but different host polymer were also reported by (Mohamad & Arof, 2007). In their work, by increase concentration of PC, the total weight loss also increases. The thermal stability of the polymer electrolytes decreased with the addition of PC plasticizer which affected to the conductivity–temperature (Fig. 3).

3.2. X-ray diffraction (XRD) analyses of A0, A16 and B8 SBEs

Fig. 6 showed XRD patterns of (a) A0 (b) A16 (c) B8 SBEs. A0 gave a strong hump at 20°. The hump centerd between $2\theta = 20°$ and 23° for A16 SBE became broadened and shifted to the higher

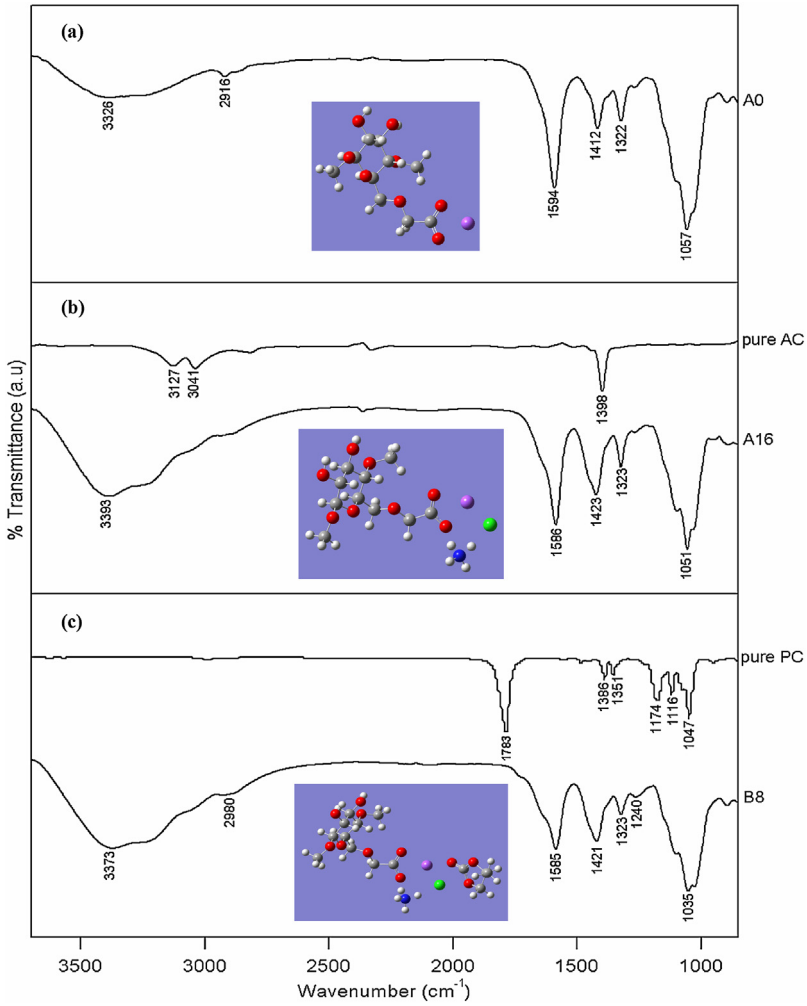

Fig. 7. IR specta, (a) A0 (b) A16 (c) B8 (Inset picture: molecular structure of compound is shown inside (a–c) whereas calculations were carried via Gaussian 09W. Red is oxygen atom, blue is nitrogen atom, green is chlorine atom, light grey is hydrogen atom, dark grey is carbon atom, purple is sodium atom) (For interpretation of the references to color in this figure legend, the reader is referred to the web version of this article.).

Bragg's angle (Ahmad & Isa, 2015b). Furthermore, the hump B8 SBE become wider than A16 SBE $2\theta = 20^{\circ}$ until 24° almost similar result reported by (Su et al., 2010; Suthanthiraraj & Vadivel, 2012), where the addition of plasticizer has greatly decreased the intensity, thereby increasing the ionic conduction. It shows that the presence of PC reduce the crystallinity compared to A16 SBE.

3.3. *Infrared spectra (IR) analyses*

The IR analyses were studied in order to obtain the information about the structure of a molecule. The IR spectrum were used to identify the bands attributable to any functional groups. In this research, two different methods; Fourier Transform Infrared spectrometer as experimental and Gaussian 09W software as computational were used to identify the functional group present in A0, A16 and B8 SBEs. Previous reported by (Ahmad & Isa, 2015b) were discussed about FTIR complexation of SBE system. They found that the characteristic bands of A0 appeared at 3700 cm^{-1} and 900 cm^{-1}. The bands at ~3500–3000 cm^{-1}, 2980–2878 cm^{-1} were allocated to the O—H stretching of hydrogen bonding and the —CH stretching region, respectively. The wavenumber of ~1594 cm^{-1}, ~1412 cm^{-1} and ~1322 cm^{-1} were corresponded to the asymmetrical COO— stretching of the carboxylate anion, $—CH_2$ scissoring and —OH bending vibration, respectively which comparable to the previous study by (Indran et al., 2014; Su et al., 2010; Zhang et al., 2014; Halim, Majid, Arof, Kajzar, & Pawlicka, 2012; Pushpamalar, Langford, Ahmad, & Lim, 2006; Silvertein, Webster, & Kiemle, 2005).

Based on previous work done by (Ahmad & Isa, 2015a), mobile ionic carrier in CMC-AC system is cation. Du and researchers have proven that H^+ is the ion which conducting species in chitosan-NH_4Cl sample and the proton conduction of polymer electrolyte film occurs by Grotthus mechanism (Du et al., 2010). According to (Hema et al., 2008), interaction between polymer–salt occurred between one of the four hydrogen atoms in NH_4^+ ions can easily be dissociated under the influence of a dc electric field.

Refer to Fig. 7(c), the band at 1240 cm^{-1} comes from C—O stretching bond of the carbonate groups by itself and also may be due hydroxyethyl chain in the backbone of the polymer. The additional peaks in the 1450–1350 cm^{-1} range were due to scissoring and bending of the C—H bonds (Spencer & Kohl, 2011). The C=O stretching was observed at wavenumber 1783 cm^{-1}. As for pure PC, the C=O is partly adjacent in between two —O groups (Indran et al., 2014).

Using single scalling factor, 0.95 (Andersson & Uvdal, 2005), the IR spectra experiment result was compared to the Gaussian 09W program result as showed in Fig. 8. It was found that the value of wavenumber (3700–900 cm^{-1}) of infrared spectrum between these 2 methods almost the same. This work was comparable as reported by previous study (Rahmani, Ghammami, & Lashgari, 2014).

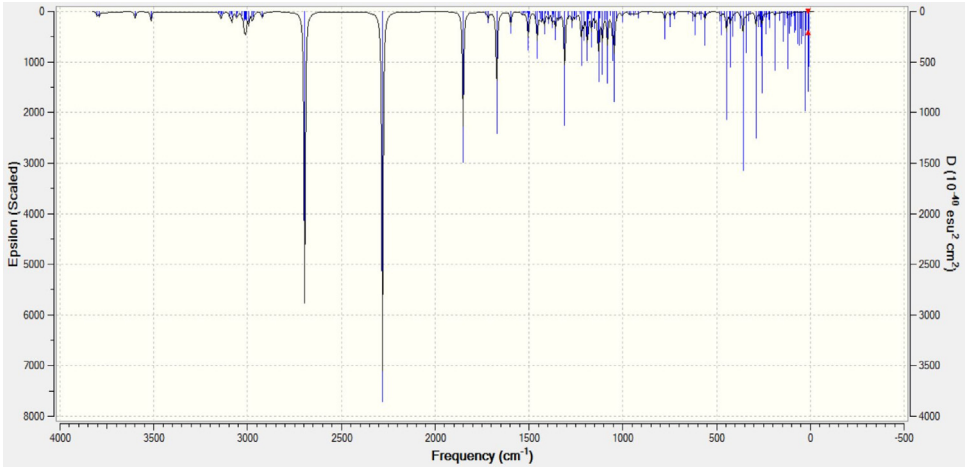

Fig. 8. Calculated infrared spectra of plasticized SBE system from Gaussian 09W program.

4. Conclusion

Un-plasticized and plasticized SBE systems based on carboxymethyl cellulose have been successfully prepared via solution cast technique. Thermal analysis by TGA/DSC showed that decomposition temperature for B8 than A16 SBE system. The decreases in the value of T_g helps increase the conductivity by the ease movement of the polymer chains. In A16 system, the highest conductivity was 1.43 10^{-3} S/cm at ambient temperature. On the other hand, the conductivity value for B8 was enhanced 1.01 $\times$ 10^{-2} S/cm. From FTIR and Gaussian results, the complexation between the SBE components is proven by the appearance of new peak at 1240 cm^{-1} for plasticized system. The changes of wavenumber showed that the interaction was completely occurred when PC was added to A16 system. All result indicates that PC plasticizer is promising candidate for conductivity enhancement of SBE system.

Acknowledgements

The authors would like to thank Ministry of Education Malaysia (MOE) for financial support through ERGS 55101 and FRGS 59271, Department of School of Fundamental Sciences, Universiti Malaysia Terengganu for the help and support throughout the research. N.H. Ahmad gratefully acknowledges MyBrain PhD for the scholarship awarded.

References

Ahmad, A., Isa, K. B. M., & Osman, Z. (2011). Conductivity and structural studies of plasticized polyacrylonitrile (PAN)—Lithium triflate polymer electrolyte films. *Sains Malaysiana*, *40*(7), 691–694.

Ahmad, N. H., & Isa, M. I. N. (2015a). Proton conducting solid polymer electrolytes based carboxymethyl cellulose doped ammonium chloride: Ionic conductivity and transport studies. *International Journal of Plastics Technology*, *18*(2), 1–11.

Ahmad, N. H., & Isa, M. I. N. (2015b). Structural and ionic conductivity studies of CMC based polymer electrolyte doped with NH_4Cl. *Advanced Materials Research*, *1107*, 247–252.

Ali, A. M. M., Yahya, M. Z. A., Bahron, H., & Subban, R. H. Y. (2007). Impedance studies on plasticized PMMA–LiX [X: CF_3SO_3, $N(CF_3SO_2)_2^-$] polymer electrolytes. *Materials Letters*, *61*, 2026–2029.

Andersson, M., & Uvdal, P. (2005). New scale factors for harmonic vibrational frequencies using the B3LYP density functional method with the triple zeta basis set 6-311+G(d,p). *The Journal of Physical Chemistry A*, *109*(12), 2937–2941.

Chai, M. N., & Isa, M. I. N. (2011). Carboxyl methylcellulose solid polymer electrolytes: Ionic conductivity and dielectric study. *Journal of Current Engineering Research*, *1*(2), 1–5.

Du, J. F., Bai, Y., Chu, W. Y., & Qiao, L. J. (2010). Synthesis and performance of proton conducting chitosan/NH_4Cl electrolyte. *Journal of Polymer Science, Part B: Polymer Physics*, *48*, 260–266.

Halim, N. F. A., Majid, S. R., Arof, A. K., Kajzar, F., & Pawlicka, A. (2012). Gellan gum-lil gel polymer electrolytes. *Molecular Crystals and Liquid Crystals*, *554*, 232–238.

Hema, M., Selvasekerapandian, S., Sakunthala, A., Arunkumar, D., & Nithya, H. (2008). Structural, vibrational and electrical characterization of PVA–NH_4Br polymer electrolyte system. *Physica B: Condensed Matter*, *403*(17), 2740–2747.

Hema, M., Selvasekarapandian, S., Arunkumar, D., Sakunthala, A., & Nithya, H. (2009). FTIR, XRD and ac impedance spectroscopic study on PVA based polymer electrolyte doped with NH4X (X = Cl, Br, I). *Journal of Non-Cystalline Solid*, *355*(2), 84–90.

Hema, M., Selvasekerapandian, S., & Hirankumar, G. (2007). Vibrational and impedance spectroscopic analysis of poly(vinyl alcohol)-based solid polymer electrolytes. *Ionics*, *13*(6), 483–487.

Indran, V. P., Syuhada Zuhaimi, N. A., Deraman, M. A., Maniam, G. P., Yusoff, M. M., Yun Hin, T.-Y., et al. (2014). An accelerated route of glycerol carbonate formation from glycerol using waste boiler ash as catalyst. *RSC Advances*, *4*(48), 25257–25267.

Johan, M. R., & Ting, L. M. (2011). Structural, thermal and electrical properties of nano manganese-composite polymer electrolytes. *Internation Journal of Electrochemical Science*, *6*, 4737–4748.

Kadir, M. F. Z. A., Teo, L. P., Majid, S. R., & Arof, A. K. (2009). Conductivity studies on plasticised PEO/chitosan proton conducting polymer electrolyte. *Materials Research Innovations*, *13*(3), 259–262.

Kamarudin, K. H., & Isa, M. I. N. (2013). Structural and DC ionic conductivity studies of carboxy methylcellulose doped with ammonium nitrate as solid polymer electrolytes. *International Journal of Physical Sciences*, *8*(31), 1581–1587.

Kumar, M., Tiwari, T., & Srivastava, N. (2012). Electrical transport behaviour of bio-polymer electrolyte system: Potato starch + ammonium iodide. *Carbohydrate Polymers*, *88*(1), 54–60.

Liu, P., Yu, L., Liu, H., Chen, L., & Li, L. (2009). Glass transition temperature of starch studied by a high-speed DSC. *Carbohydrate Polymers*, *77*(2), 250–253.

Mohamad, A. A., & Arof, A. K. (2007). Plasticized alkaline solid polymer electrolyte system. *Materials Letters*, *61*(14–15), 3096–3099.

Morales, E., & Acosta, J. L. (1997). Thermal and electrical characterization of plasticized polymer electrolytes based on polyethers and polyphosphazene blends. *Solid State Ionics*, *96*, 99–106.

Ng, L. S., & Mohamad, A. A. (2006). Protonic battery based on a plasticized chitosan–NH_4NO_3 solid polymer electrolyte. *Journal of Power Sources*, *163*(1), 382–385.

Pitawala, H. M. C., Dissanayake, M. A. K. L., Seneviratne, V. A., Mellander, B. E., & Albinson, I. (2008). Effect of plasticizers (EC or PC) on the ionic conductivity and thermal properties of the (PEO) 9LiTf:Al_2O_3 nanocomposite polymer electrolyte system. *Journal of Solid State Electrochemistry*, *12*(7–8), 783–789.

Pradhan, D. K., Choudhary, R. N. P., & Samantaray, B. K. (2008). Studies of dielectric relaxation and AC conductivity behavior of plasticized polymer nanocomposite electrolytes. *International Journal of Electrochemical Science*, *3*, 597–608.

Pradhan, D. K., Choudhary, R. N. P., Samantaray, B. K., Karan, N. K., & Katiyar, R. S. (2007). Effect of plasticizer on structural and electrical properties of polymer nanocompsoite electrolytes. *International Journal of Electrochemical Science*, *2*, 861–871.

Pushpamalar, V., Langford, S. J., Ahmad, M., & Lim, Y. Y. (2006). Optimization of reaction conditions for preparing carboxymethyl cellulose from sago waste. *Carbohydrate Polymers*, *64*, 312–318.

Rahmani, S., Shanti, R., & Morris, E. (2014). Structural properties, density functional theory (DFT), natural bond orbital and energy calculations for the fluorous compound $C_{18}H_{10}F_{11}BrN_4O$. *Fluorine Notes*, *5*(96). http://notes.fluorine1.ru/public/2014/5_2014/letters/letter2.html.

Rajendran, S., Sivakumar, M., & Subadevi, R. (2003). Effect of salt concentration in poly(vinyl alcohol)-based solid polymer electrolytes. *Journal of Power Sources*, *124*(1), 225–230.

Ramesh, S., Shanti, R., & Morris, E. (2012). Studies on the thermal behavior of CS:LiTFSI:[Amim] Cl polymer electrolytes exerted by different [Amim] Cl content. *Solid State Sciences*, *14*(1), 182–186.

Ramesh, S., & Arof, A. K. (2001). Structural, thermal and electrochemical cell characteristics of poly(vinyl chloride)-based polymer electrolytes. *Journal of Power Sources*, *99*, 41–47.

Rani, M., Rudhziah, S., Ahmad, A., & Mohamed, N. (2014). Biopolymer electrolyte based on derivatives of cellulose from kenaf bast fiber. *Polymers*, *6*(9), 2371–2385.

Ravi, M., Pavani, Y., Kiran Kumar, K., Bhavani, S., Sharma, A. K., & Narasimha Rao, V. V. R. (2011). Studies on electrical and dielectric properties of PVP:$KBrO_4$ complexed polymer electrolyte films. *Materials Chemistry and Physics*, *130*(1–2), 442–448.

Silvertein, Robeth M., Webster, Francis X., & Kiemle, David J. (2005). *Spectrometric identification of organic compounds* (7th ed., pp. 74–101). New York, NY: John Wiley & Sons.

Rozali, M. L. H., & Isa, M. I. N. (2014). Electrical behaviour of carboxy methyl cellulose doped adipic acid solid biopolymer electrolyte. *International Journal of Material Sciences*, *4*(2), 59.

Samsudin, A. S., & Isa, M. I. N. (2013). Conductivity and transport properties study of plasticized carboxymethyl cellulose (CMC) based solid biopolymer electrolytes (SBE). *Advanced Materials Research*, *856*, 118–122.

Samsudin, A. S., Lai, H. M., & Isa, M. I. N. (2014). Biopolymer materials based carboxymethyl cellulose as a proton conducting biopolymer electrolyte for application in rechargeable proton battery. *Electrochimica Acta*, *129*, 1–13.

Saroj, A. L., & Singh, R. K. (2012). Thermal, dielectric and conductivity studies on PVA/ionic liquid [EMIM][$EtSO_4$] based polymer electrolytes. *Journal of Physics and Chemistry of Solids*, *73*(2), 162–168.

Sekhar, P. C., Kumar, P. N., & Sharma, A. K. (2012). Effect of plasticizer on conductivity and cell parameters of (PMMA + $NaClO_4$) polymer electrolyte system. *Journal of Applied Physics*, *2*(4), 1–6.

Shukur, M. F., Ithnin, R., & Kadir, M. F. Z. (2014). Electrical properties of proton conducting solid biopolymer electrolytes based on starch–chitosan blend. *Ionics*, *20*(7), 977–999.

Sohaimy, M. I. H., & Isa, M. I. N. (2015). Conductivity and dielectric analysis of cellulose based solid polymer electrolytes doped with ammonium carbonate (NH_4CO_3). *Applied Mechanics and Materials*, *719–720*, 67–72.

Spencer, T. J., & Kohl, P. A. (2011). Decomposition of poly(propylene carbonate) with UV sensitive iodonium salts. *Polymer Degradation and Stability*, *96*(4), 686–702.

Sreenivasachari, A. (2013). Preparation, Investigation and discharge characteristics of (PVC + PC + $NaClO_4$) Polymer Electrolyte Systems. *International Journal of Applied Research and Studies*, *2*, 1–12.

Su, J. F., Huang, Z., Yuan, X. Y., Wang, X. Y., & Li, M. (2010). Structure and properties of carboxymethyl cellulose/soy protein isolate blend edible films crosslinked by Maillard reactions. *Carbohydrate Polymers*, *79*(1), 145–153.

Suthanthiraraj, S. A., & Vadivel, M. K. (2012). Effect of propylene carbonate as a plasticizer on $(PEO)_{50}AgCF_3SO_3$:SnO_2 nanocomposite polymer electrolyte. *Applied Nanoscience*, *2*, 239–246.

Taib, N. U., & Idris, N. H. (2014). Plastic crystal-solid biopolymer electrolytes for rechargeable lithium batteries. *Journal of Membrane Science*, *468*, 149–154.

Wright, P. V. (May 1975). Electrical conductivity in ionic complexes of poly(ethylene oxide). *British Polymer Journal*, *7*, 319–327.

Yokota, S., Ueno, T., Kitaoka, T., & Wariishi, H. (2007). Molecular imaging of single cellulose chains aligned on a highly oriented pyrolytic graphite surface. *Carbohydrate Research*, *342*(17), 2593–2598.

Zhang, J., Liping, Y., Pu, H., Zhihong, L., Bingsheng, Q., Zhang, B., et al. (2014). Taichi-inspired rigid-flexible coupling cellulose-supported solid polymer electrolyte for high-performance lithium batteries. *Scientific Reports*, *4*, 6272.

Zhang, L., Liu, Z., Cui, G., & Chen, L. (2015). Biomass-derived materials for electrochemical energy storages. *Progress in Polymer Science*, *43*, 136–164.